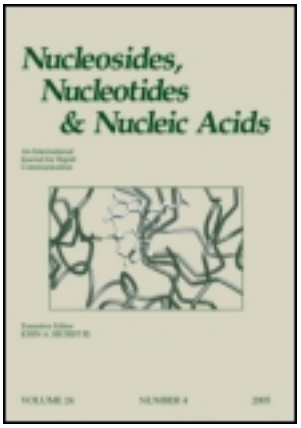

Nucleosides, Nucleotides and Nucleic Acids

Publication details, including instructions for authors and subscription information:
http://www.tandfonline.com/loi/lncn20

Synthesis, Crystal Structure, and in Vitro Biological Evaluation of C-6 Pyrimidine Derivatives: New Lead Structures for Monitoring Gene Expression in Vivo

Miljen Martić [a], Lucile Pernot [b], Yvonne Westermaier [b], Remo Perozzo [b], Tatjana Gazivoda Kraljević [c], Svjetlana Krištafor [c], Silvana Raić-Malić [c], Leonardo Scapozza [b] & Simon Ametamey [a]

[a] Center for Pharmaceutical Science of ETH, PSI and USZ, ETH Zürich, Zürich, Switzerland

[b] Pharmaceutical Biochemistry group, School of Pharmaceutical Sciences, University of Geneva, University of Lausanne, Geneva, Switzerland

[c] Department of Organic Chemistry, Faculty of Chemical Engineering and Technology, University of Zagreb, Zagreb, Croatia

Published online: 27 May 2011.

To cite this article: Miljen Martić , Lucile Pernot , Yvonne Westermaier , Remo Perozzo , Tatjana Gazivoda Kraljević , Svjetlana Krištafor , Silvana Raić-Malić , Leonardo Scapozza & Simon Ametamey (2011): Synthesis, Crystal Structure, and in Vitro Biological Evaluation of C-6 Pyrimidine Derivatives: New Lead Structures for Monitoring Gene Expression in Vivo, Nucleosides, Nucleotides and Nucleic Acids, 30:4, 293-315

To link to this article: http://dx.doi.org/10.1080/15257770.2011.581258

Nucleosides, Nucleotides and Nucleic Acids, 30:293–315, 2011

ISSN: 1525-7770 print / 1532-2335 online
DOI: 10.1080/15257770.2011.581258

SYNTHESIS, CRYSTAL STRUCTURE, AND IN VITRO BIOLOGICAL EVALUATION OF C-6 PYRIMIDINE DERIVATIVES: NEW LEAD STRUCTURES FOR MONITORING GENE EXPRESSION IN VIVO

Miljen Martić,[1] Lucile Pernot,[2] Yvonne Westermaier,[2] Remo Perozzo,[2] Tatjana Gazivoda Kraljević,[3] Svjetlana Krištafor,[3] Silvana Raić-Malić,[3] Leonardo Scapozza,[2] and Simon Ametamey[1]

[1]Center for Pharmaceutical Science of ETH, PSI and USZ, ETH Zürich, Zürich, Switzerland
[2]Pharmaceutical Biochemistry group, School of Pharmaceutical Sciences, University of Geneva, University of Lausanne, Geneva, Switzerland
[3]Department of Organic Chemistry, Faculty of Chemical Engineering and Technology, University of Zagreb, Zagreb, Croatia

□ *Novel C-6 substituted pyrimidine derivatives are good substrates of herpes simplex virus type 1 thymidine kinase (HSV1-TK). Enzyme kinetic experiments showed that our lead compound, N-methyl DHBT (N-methyl-6-(1,3-dihydroxyisobutyl) thymine; N-Me DHBT), is phosphorylated at a similar rate compared to "gold standard" 9-[4-fluoro-3-(hydroxymethyl)butyl]guanine, FHBG, ($K_m = 10 \pm 0.3\ \mu M$; $k_{cat} = 0.036 \pm 0.015\ sec^{-1}$). Additionally, it does not show cytotoxic properties on B16F1 cells up to a concentration of 10 mM. The x-ray analysis of the crystal structures of HSV1-TK with N-Me DHBT and of HSV1-TK with the fluorinated derivative N-Me FHBT confirmed the binding mode predicted by docking studies and their substrate characteristics. Moreover, the crystal structure of HSV1-TK with N-Me DHBT revealed an additional water-mediated H-bond interesting for the design of further analogues.*

Keywords C-6 pyrimidine derivatives; N-Me DHBT; HSV1-TK; positron emission tomography

INTRODUCTION

A noninvasive imaging modality, such as positron emission tomography (PET), offering the possibility of monitoring the location, magnitude,

Received 21 February 2011; accepted 11 April 2011.
M. M. and L. P. contributed equally to this article.
We thank the x06sa and the x06da beamline scientists at the SLS for their help in collecting x-ray data. L. P. was first a Biomedizin-Naturwissenschaft-Forschung fellow and subsequently a recipient of a grant from the Novartis Consumer Health Foundation. This work was supported by the grant SNF No. 3100A0-113830/1.
Address correspondence to Leonardo Scapozza, Pharmaceutical Biochemistry Group, School of Pharmaceutical Science, University of Geneva, University of Lausanne, Quai Ernest Ansermet 30 CH-1211 Geneva 4, Switzerland. E-mail: leonardo.scapozza@unige.ch

and duration of gene expression over time is critically important for the application of gene therapy to human beings. To be considered as suitable agents for monitoring herpes simplex virus type 1 thymidine kinase (HSV1-TK) expression in vivo by PET, compounds have to fulfill several requirements[1]: good catalytic efficacy for HSV1-TK, high specificity toward the HSV1-TK enzyme, low specificity toward other human enzymes, low cytotoxicity in normal and TK-transfected cells, a suitable structure for radiolabeling and favorable pharmacokinetics. Non-fluorinated acyclic nucleoside analogues are known to be potent anti-herpes virus agents.[2,3] The most efficient ones, aciclovir (ACV) and ganciclovir (GCV) possess low host toxicity and are active against herpes simplex virus type 1 and type 2.[3,4] The selectivity of these acyclic nucleoside analogues is due, in part, to the fact that they are only phosphorylated in virus-infected cells, where a virus specific thymidine kinase of low substrate specificity converts the nucleoside analogues to their monophosphate derivatives. Our investigations were prompted by the need to develop PET imaging agents which lack the disadvantages of already existing reporter probes of HSV1-TK, such as 9-[4-[^{18}F]fluoro-3-(hydroxymethyl)-butyl]guanine ([^{18}F]FHBG), which shows cytotoxicity and unfavorable pharmacokinetics (Figure 1). Previous results with a C-6 substituted pyrimidine derivative, 6-(2,3-dihydroxypropyl)-5-[^{18}F]fluoromethyl-(1H,3H)-pyrimidine-2,4-dione ([^{18}F]fluoromethyl-HHT) in a murine melanoma cell line B16 F1 tumor model, showed that [^{18}F]fluoromethyl-HHT is indeed far superior to [^{18}F]FHBG, due to

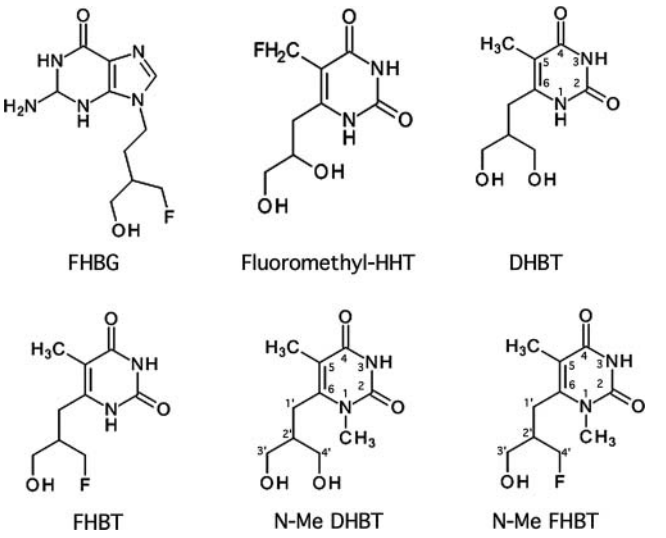

FIGURE 1 Structure of FHBG and C-6 alkylated pyrimidine derivatives. The compound N-Me DHBT bears a methyl substitution in the N-1 and the acyclic sugar extends from the carbon C-6.

a greater sensitivity and contrast, as well as lower levels of abdominal background radioactivity.[5] However, it has the disadvantage of in vivo defluorination. In a previous work,[6,7] we described the lead compound DHBT (6-(1,3-dihydroxyisobutyl)thymine) and discussed its advantages over existing compounds. Those promising results prompted us to further explore the chemical space of novel C-6 thymine derivatives and the substrate acceptability of HSV1-TK. Unlike existing PET reporter probes that bear aliphatic side chains or sugar moieties in the N-1 position of purine or pyrimidine, we intend to evaluate new fluorinated compounds that are C-6 alkylated pyrimidine derivatives. As we aimed to improve the in vivo stability of the new compound by first placing the ^{18}F radiolabel in the acyclic side chain extending from the C-6 position of the thymine ring, we introduced a methyl group in the N-1 position in order to circumvent the intramolecular cyclization of the compound (Figure 1).

Herein, we describe a docking study on a N-1 methylated derivative, a synthesis of the lead compound N-Me DHBT (N-methyl-6-(1,3-dihydroxyisobutyl)thymine) and the x-ray structures of HSV1-TK in complex respectively, with N-Me DHBT and with the fluorinated derivative N-Me FHBT, respectively (Figure 1). Additionally, we provide the binding affinity of N-Me DHBT to HSV1-TK, its kinetic turnover constant and an evaluation of the effect on the proliferation of HSV-1 TK transduced and nontransduced B16F1 cell lines.

EXPERIMENTAL

Docking Studies Using GOLD

The human thymidine kinase (PDB entry code 1W4R) and HSV1-TK (PDB entry code 1VTK) x-ray structures were retrieved from the Protein Data Bank in pdb format. For each structure, monomer A was kept and hydrogens and Gasteiger charges added using Sybyl 7.2 (Tripos Inc., St. Louis, MO, USA). Then, both structures were stored in mol2 format. For the putative ligands of hTK1 and HSV1-TK, hydrogens and Gasteiger-Huckel partial charges were assigned. Subsequently, the energy of each ligand was minimized using the Powell method with an initial simplex optimization. The termination criterion was set to a gradient of 0.05 kcal/mol × A and the number of maximal iterations to 1000.

Standard GOLD parameters were applied, except for the definition of the active site, where an origin was defined as the center of a sphere with a 6.5 Å radius. For hTK1, its coordinates were 37.67, 93.58, and −19.48 for x, y, and z, respectively. This corresponds to the centroid (center of mass) of dTTP (thymidine triphosphate) in subunit A of 1W4R. For HSV1-TK,

these centroid coordinates were set to 39.50, 16.73, and 31.94 (reflecting the centroid of dTMP (thymidine monophosphate) in subunit A of 1VTK), respectively. For each compound, 10 GOLD runs were done. The docking protocol was validated by redocking several ligands (thymidine, penciclovir (PCV), ganciclovir (GCV), and DHBT) into the corresponding x-ray crystal structures.

Synthesis of the Lead Compound N-Me DHBT

The synthesis of N-Me DHBT is shown in Figure 2.

The ^{1}H NMR and ^{13}C NMR spectra were recorded on a 300 MHz Varian Gemini 2000 (Varian Inc., USA) or a Bruker 400 MHz spectrometer (Bruker, Germany) with tetramethylsilane as an internal standard. All data were recorded in DMSO-d_6 at 298 K. Chemical shifts were referenced to the residual solvent signal of DMSO at δ 2.50 ppm for ^{1}H and δ 39.50 ppm for ^{13}C. Individual resonances were assigned on the basis of their chemical shifts, signal intensities, multiplicity of resonances, and H-H coupling constants. Chemical shifts, δ, are reported in parts per million referred to TMS, and signals are expressed as s (singlet), d (doublet), t (triplet), q (quartet), m (multiplet), or br (broad). Coupling constants (J) are expressed in Hz. Mass spectroscopy analysis was performed with a Micromass Quattro micro TM API LC-ESI or a LCT Premier ESI-TOF from Waters (France). The TLC was done on Merck silica gel 60 F254 precoated plates. Compound was visualized under ultraviolet (UV) light (254 nm). The silica gel used for column chromatography was silica gel 60, particle size 0.040–0.063 mm (230–400 mesh ASTM), Fluka, Germany. Evaporations were performed using a Büchi Rotavapor R-215 system at 40°C (Büchi, Switzerland).

2,4-Dichloro-5,6-dimethylpyrimidine (2)

A mixture of 2,4-dihydroxy-5,6-dimethylpyrimidine **1** (6.33 g, 45 mmol) and $POCl_3$ (30 ml, 328 mmol) was heated under reflux for 4 hours. Excess of $POCl_3$ was then removed under reduced pressure and the residue was added to ice, washed with ether, and dried over sodium sulphate. The crude product was recrystallized from ethanol to give **2** (7.54 g, 94.3%, m.p. 70–71°C); ($C_6H_6N_2Cl_2$), $R_f = 0.65$ (n-hexane/EtOAc = 5/1).

^{1}H NMR (DMSO-d_6): 2.26 (s, 3H, CH_3), 2.47 (s, 3H, CH_3).

^{13}C NMR (DMSO-d_6): δ 155.24 (C-2), 171.48 (C-4), 127.74 (C-5), 160.54 (C-6), 22.83 (CH_3), 14.40 (CH_3).

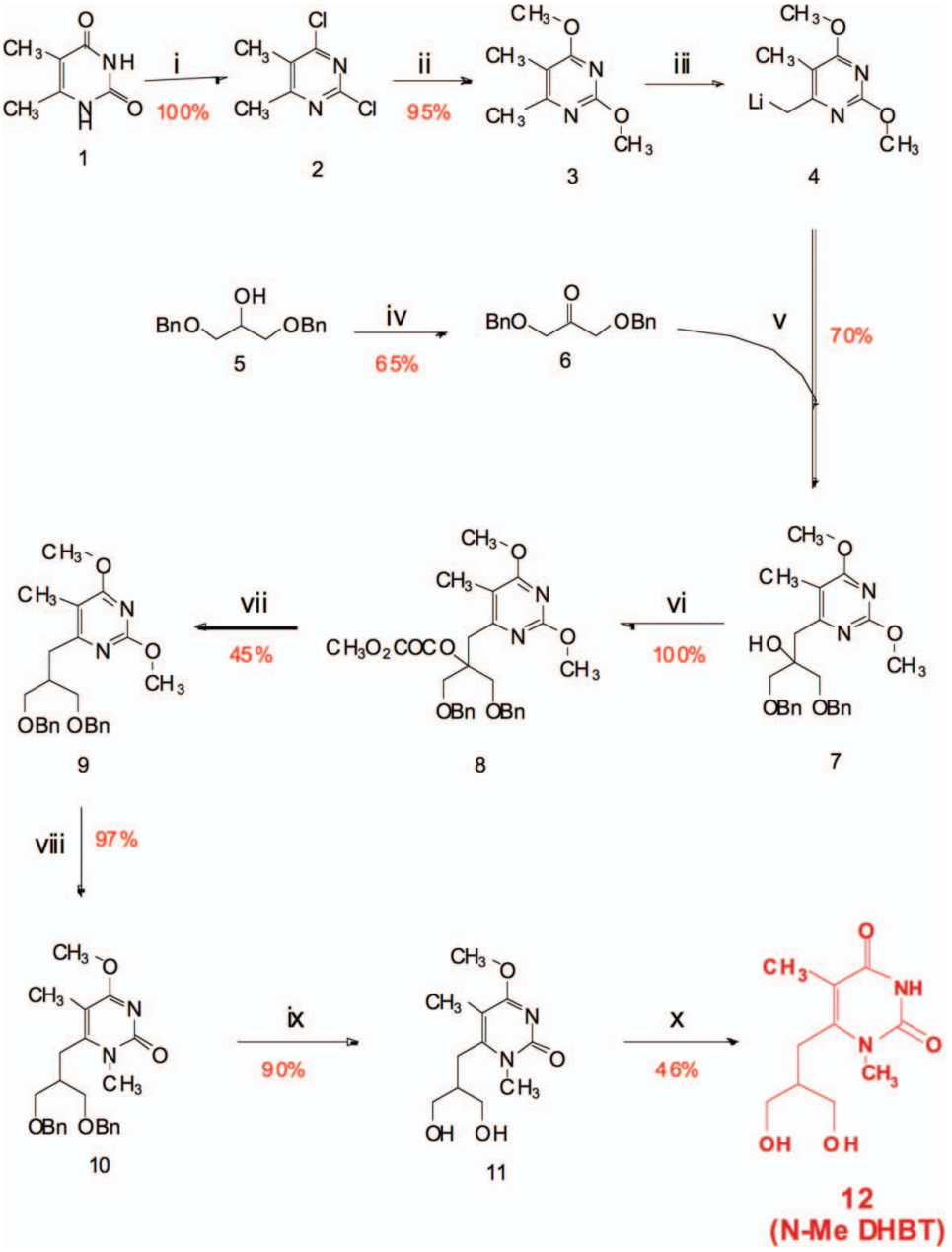

FIGURE 2 Synthetic pathway to the novel lead compound N-Me DHBT. Reagents and conditions: (i) $POCl_3$, reflux; (ii) $NaOCH_3$, MeOH; (iii) LDA, THF; (iv) N-chlorosuccinimide, Et_3N, toluene; (v) −55°C, THF; (*vi*) $C_3H_3ClO_3$, DMAP, CH_3CN; (vii) Bu_3SnH, AIBN, Toluene; (viii) CH_3I; (ix) −78°C, BCl_3, CH_2Cl_2; (x) AcCl, H_2O; NH_3, MeOH. Synthetic yields for each reaction ranged from 45 to 100% and are reported. (Color figure available online.)

2,4-Dimethoxy-5,6-dimethylpyrimidine (3)

2 (7.54 g, 42.6 mmol) was added to a solution of sodium (2 g, 87.0 mol) in methanol (50 ml). The reaction mixture was refluxed for 6 hours. The solvent was evaporated and water was added to dissolve NaCl. The oily layer was extracted with dichloromethane, dried over sodium sulphate and concentrated under reduced pressure. The residue was kept in refrigerator and gave colorless crystals of **3** (7.10 g, 99.1%, m.p. 39–40°C).

^{1}H NMR (DMSO-d_6): 1.98 (s, 3H, CH_3), 2.29 (s, 3H, CH_3); 3.82 (s, 3H, OCH_3), 3.87 (s, 3H, CH_3).

^{13}C NMR (DMSO-d_6): δ 162.10 (C-2), 168.67 (C-4), 107.25 (C-5), 165.67 (C-6), 53.96 (OCH_3), 53.74 (OCH_3), 21.46 (CH_3), 9.67 (CH_3).

1,3-Bis(benzyloxy)propan-2-one (6)

N-Chlorosuccinimide (18.0 g, 134.8 mmol) was suspended in dry toluene (210 ml), and the mixture was cooled in a dry ice bath. Dimethyl sulfide (15 ml, 204.2 mmol) was added, and the mixture was cooled to −25°C in a dry ice-CH_2Cl_2 bath. 1,3-bis(benzyloxy)-2-propanol **5** (25.0 g, 91.8 mmol) in toluene (21 ml) was added to the mixture, and the mixture was kept under argon for 4 hours. Triethylamine (100 ml, 717.5 mol) was added and the reaction was allowed to warm until reaching room temperature. After 30 minutes of stirring at room temperature, the solution was passed through a filter paper. The residue was washed with a diethyl ether (250 ml). The filtrate and the washings were combined, neutralized with 5% aqueous HCl to pH 7, washed with a saturated NaCl solution (3 × 50 ml) and then with water (3 × 50 ml), and finally dried over sodium sulphate. The solvent was removed in vacuum and the resulting oil was purified by column chromatography (n-hexane/EtOAc = 4/1) to give 13.5 g (54.4% yield) of compound **6** ($C_{17}H_{18}O_3$). m.p. 40°C.

MS m/z: 270.1 (M^+).

^{1}H NMR (DMSO-d_6): 7.23 (10H, Ph), 4.46 (s, 4H, CH_2Ph), 4.13 (s, 4H, CH_2O).

6-(3-Benzyloxy)-2-benzyloxymethyl-2-hydroxypropyl)-2,4-dimethoxy-5-methylpyrimidine (7)

LDA (1.5 M, 45 ml, 113 mmol) was added dropwise to a solution of 2,4 dimethoxy-5,6-dimethylpyrimidine **3** (7.50 g, 44.6 mmol) in THF (90 ml) at −70°C. The temperature was raised to −55°C, and the solution was stirred for 30 minutes. **6** (12.00 g, 44.4 mmol) in THF (65 ml) was added dropwise

to this solution and stirring was continued for 2.5 hours while the temperature was maintained at −55°C. The solution was neutralized by the addition of AcOH to pH 7 and then the temperature was raised to 25°C and the solvent removed. The residue was partitioned between AcOEt and H_2O. The organic layer was separated, dried over sodium sulphate and removed by evaporation. The residue was isolated by chromatography on silica gel column, eluting with *n*-hexane/EtOAc = 3/1. The desired fractions were concentrated in vacuum to afford compound **7** in 59% yield (1.25 g).

MS m/z: 439.3 (M^+).

^{1}H NMR (DMSO-d_6): 7.28 (10H, Ph), 5.09 (s, 1H, OH), 4.48 (s, 4H, CH_2Ph), 3.87 (s, 2H, CH_2O), 3.76 (s, 3H, OCH_3), 3.44 (s, 3H, OCH_3), 2.83 (s, 2H, CH_2), 1.99 (s, 3H, CH_3).

6-[3-Benzyloxy-2-(benzyloxymethyl)propyl]-2,4-dimethoxy-5-methylpyrimidine (9)

Methyl oxalyl chloride (5.9 ml, 63.7 mmol) was added to a mixture of 6-3-(Benzyloxy-2-benzyloxymethyl-2-hydroxypropyl-2,4-dimethoxy-5-methylpyrimidine **7** (6.00 g, 13.7 mmol) and 4-(dimethylamino) pyridine (DMAP, 3.7 g, 29.6 mmol) in dry CH_3CN (50 ml) at 0°C under argon. The mixture was stirred for 14 hours under argon at room temperature and then diluted with EtOAc (400 ml). The mixture was washed successively with a saturated aqueous $NaHCO_3$ solution (120 ml) and H_2O (120 ml). The separated organic phase was dried over sodium sulphate and the solvent was removed under reduced pressure. The residue was co-evaporated twice with dried toluene (40 ml) to afford the methyl oxalyl ester **8**. MS m/z: 481 (M+).

A mixture of Bu_3SnH (9.0 ml, 36 mmol) and 2,2′-azobis (isobutyronitrile) (AIBN; 180 mg, 1.1 mmol) in dry toluene (50 ml) was added to a solution of **8** in dry toluene (130 ml) under an argon atmosphere. The mixture was heated at 110°C for 3 hours and the solvent was removed by evaporation under reduced pressure. The residue was purified by column chromatography (mixture of n-hexane/EtOAc = 4/1 as mobile phase) to afford 2.77 g of 6-[3-benzyloxy-2-[(benzyloxymethyl)propyl]thymine **9** in 48% yield.

MS m/z: 423.3 (M^+).

^{1}H NMR (DMSO-d_6): 7.29 (10H, Ph), 4.42 (s, 4H, CH_2Ph), 3.87 (s, 3H, OCH_3), 3.79 (s, 3H, OCH_3), 3.43 (d, 4H, OCH_2), 2.68 (d, 2H, CH_2), 1.97 (s, 3H, CH_3).

6-[3-(Benzyloxy-2-(benzyloxymethyl)propyl]-4-methoxy-1,5-dimethylpyrimidin-2(1H)-one (10)

A mixture of **9** (3.6 g, 7.57 mol) and CH_3I (50 ml, 803 mol) was refluxed at 50°C for 4 days and evaporated to dryness. The raw product was purified on silica column (n-pentane/EtOAc = 1/1) to afford 3.5 g of pure **10** in 97% yield.

MS: 423.3 (M^+)

^{1}H NMR ($CDCl_3$): 7.24 (m, 10H, Ph), 4.40 (q, 4H, CH_2), 3.88 (s, 3H, CH_3), 3.45 (s, 3H, CH_3), 3.42 (d, 4H, CH_2), 2.78 (d, 2H, CH_2), 2.10 (m, 1H, CH), 2.95 (s, 3H, CH_3).

6-[3-Hydroxy-2-(hydroxymethyl)propyl]-4-methoxy-1,5-dimethylpyrimidin-2(1H)-one (11)

A mixture of **10** (3.2 g, 7.57 mmol) in dry CH_2Cl_2 (40 ml) was cooled to −78°C. BCl_3 (1 M in CH_2Cl_2, 35 ml, 35 mol) was added via a syringe and under argon. The mixture was stirred at −78°C for 2 hours and then the temperature was raised to −40°C. A mixture of CH_2Cl_2/MeOH (1/1; 100 ml) was added and the cooling bath was removed. The solution was neutralized with a saturated $NaHCO_3$ solution to pH 7 and stirred for additional 30 minutes. The water layer was separated and solvent was removed under reduced pressure to give 1.65 g of pure **11** in 90% yield.

MS m/z: 243.3 (M^+).

^{1}H NMR ($CDCl_3$): 1.96 (s, 3H, CH_3), 2.01 (br, 1H, CH), 2.83 (m, 2H, CH_2), 3.47 (s, 3H, CH_3), 3.58 (m, 4H, CH_2 + CH_2), 3.87 (s, 3H, OCH_3).

6-[3-Hydroxy-2-(hydroxymethyl)propyl]-1,5-dimethylpyrimidin-2,4(1H,3H)-dione (N-Me DHBT) (12)

A solution of **11** (3.0 g, 12.4 mmol) dissolved in acetyl chloride (10 ml) and containing a few drops of water was stirred at reflux for 48 hours. The solvent was removed under reduced pressure and the residue was dissolved in saturated methanolic ammonia (50 ml) stirred at room temperature for additional 4 hours, and then evaporated to dryness. The product was purified on a silica column ($CHCl_3$/i-PrOH = 4/1) to give pure N-Me DHBT (1.3 g) in 46% yield.

MS m/z: 229.17 (M^+).

^{1}H NMR ($CDCl_3$): 1.86 (s, 3H, CH_3), 1.96 (m, 1H, CH), 2.73 (d, 2H, CH_2), 3.35 (s, 3H, CH_3), 3.58 (m, 4H, CH_2 + CH_2).

^{13}C NMR ($CDCl_3$): 10.96 (CH_3), 28.08 ($C_{1'}$); 31.80 (N-CH_3), 41.65 ($C_{2'}$), 61.15 ($C_{3'}$,$C_{4'}$), 109.44 (C_5), 153.85 (C_2, C_4).

HPLC Assay for Monitoring the Phosphorylation of N-Me DHBT

A previously published protocol was used.[8,9] Briefly, reactions were carried out in a final volume of 75 μl containing H_2O (58.2 μl), 1 M Tris buffer, pH 7.4 (3.75 μl), 100 mM ATP (3.75 μl), 100 mM $MgCl_2$ (3.75 μl), 1 mM N-Me DHBT (3.75 μl), and 2–10 μg of HSV1-TK. The reaction were carried at 37°C and were stopped by addition of 2.5 mM EDTA (675 μl) at time-points 10, 20, 30, 45, 60, and 90 minutes. The obtained mixture was then injected into an HPLC column for the analysis (column, C-18; solvent, 0.2 M NaH_2PO_4, 25 mM tetrabutylammonium hydrogen sulphate, 3% methanol; flow 1.1 ml/min; detection: diode array detector). The formation of the monophosphorylated compound as well as ADP, was monitored qualitatively. Two different blank reactions (no enzyme or no substrate) were run concurrently to account for the occurring minimal reaction, independent of ATP hydrolysis. All reactions were performed in triplicates.

Determination of K_m and k_{cat} by Spectrophotometric Assays

The K_m and k_{cat} values were determined as described in the literature.[9,10] Reaction mixtures with a final volume of 75 μl containing 50 mM Tris buffer pH 7.2, 1 mM 1,4-dithio-DL-threitol, 0.21 mM phosphoenolpyruvate, 2.5 mM $MgCl_2$, 5 mM ATP, 0.18 mM NaDH, 0.8 μg pyruvate kinase, 0.5 μg L-lactate dehydrogenase, and different concentrations of the substrate (0.01 mM, 0.05 mM, 0.1 mM, 0.25 mM, 0.5 mM, 1 mM) were incubated at 37°C. Two minutes later, 5 μg of HSV1-TK were added in order to initiate the reaction. The changes in absorbance at 340 nm corresponding to ADP formation of the TK-dependent reaction at 37°C were monitored during 20 minutes. The data presented are the results of the measurements performed in triplicates. Control experiments were performed in order to take into account the spontaneous hydrolysis of ATP under the experimental conditions.

Cell Proliferation Assay

Confluent B16F1 cells stably transduced with HSV1-TK (B16F1 HSV1-TK+) and wild-type cells (B16F1 wt) were trypsinisated and resuspended in 10 ml of fresh RPMI 1640 medium supplemented with 10% fetal calf serum and 1% antibiotic PSF solution. The cell concentration for a 1:1 dilution with trypan blue was determined using a Neubauer's counting chamber. The suspension was diluted with the medium to a final concentration of 20,000 cells per milliliter.

The protocol used was similar to one previously published.[9] Of the suspension, 100 μl (2000 cells) were seeded in each well of a 96 well Nunclon surface plate from Nunc (ThermoFisher Scientific, Denmark). After 1.5 hours of incubation at 37°C, the cells were attached to the bottom of the

wells. 100 μl of sterile solutions of ganciclovir (GCV) and N-Me DHBT in RPMI 1640 were added to the cells leading to final substrate concentrations of 0.05, 0.1, 1, 5, 10, 50, 100, 500, and 1000 μM. All samples were prepared in triplicates for each cell line. The wells without thymidine analogue allow calculating the standard value of 100% of cell growth. The plates were incubated for 3.5 days at 37°C in the presence of 5% CO_2. Viability of the cells was measured by a colorimetric assay using the XTT labeling reagent (sodium 3′-[1-(phenylaminocarbonyl)- 3,4-tetrazolium]-bis(4-methoxy-6-nitro)benzene sulfonic acid hydrate). 50 μl of the XTT reagent were added to each well.[11,12] After 9 hours of incubation at 37°C in the presence of 5% CO_2, the number of viable cells in each well was determined by a colorimetric UV absorption measurement of the converted XTT with a plate reader at a wavelength of 450 nm. To account for the absorbance due to the presence of both varying numbers of cells and nonmetabolized XTT, the optical density (OD) at a reference wavelength of 750 nm was subtracted.[11,12]

Protein Expression, Purification, and Crystallization

The HSV1-TK was expressed as a GST-TK fusion protein and further purified as HSV1-TK by using glutathione affinity chromatography following protocols that have been reported earlier.[13,14]

Best crystals of HSV1-TK were obtained at 23°C (296 K) with the vapor diffusion technique using the geometry of the sitting-drop. Crystals grew in 0.9–1.2 M Li_2SO_4, 1 mM DTT and 0.1 M HEPES buffer at pH 7.5–8.0.[14] Crystals of HSV1-TK were soaked for 30 minutes in the high salt crystallization solution to which 5 mM of either N-methyl-6-(1,3-dihydroxyisobutyl)thymine, N-Me DHBT, or N-Me FHBT were added, respectively.

Prior to data collection, the crystals were immerged for a short time in the crystallization buffer containing 30% (v/v) glycerol and were subsequently frozen in a gaseous nitrogen stream at 100 K. The crystals belong to the orthorhombic space group $C222_1$ with unit cells parameters $a = 113.0$ Å, $b = 117.4$ Å, $c = 107.8$ Å, $\alpha = \beta = \gamma = 90°$ for the HSV1-TK:N-Me DHBT crystal and $a = 114.2$ Å, $b = 118.3$ Å, $c = 108.9$ Å, $\alpha = \beta = \gamma = 90°$ for the HSV1-TK:N-Me FHBT crystal.

Data Collection, Structure Solution, and Refinement

The x-ray data set of HSV1-TK:N-Me DHBT crystal was collected at the beam-line x06sa, equipped with the pixel-detector PILATUS and tuned at a wavelength of 1 Å, at the synchrotron Swiss Light Source (Villigen, Switzerland). An angular increment between the diffraction images of 1° and a crystal-to-detector distance of 300 mm were chosen. The x-ray data set of HSV1-TK:N-Me FHBT crystal was collected at the synchrotron Swiss Light

Source on the beam-line x06DA, equipped with the MAR CCD detector and tuned at a wavelength of 1 Å. The crystal-to-detector distance was fixed at 255 mm and 0.5° was chosen as an angular increment between the diffraction images. The datasets were obtained from a single crystal, respectively. Raw diffraction images were indexed and integrated with MOSFLM7.0.1.[15] Data scaling, merging, and reduction was carried out with programs of the CCP4 suite.[16] Relevant statistics are given in Table 2.

The structure of HSV1-TK containing the substrate analogue N-Me DHBT was determined by molecular replacement with the program PHASER[17] using the model of HSV1-TK complexed with the substrate analogue 6-(1,3-dihydroxyisobutyl)thymine, DHBT (1E2P) as a search probe. Before starting the molecular replacement procedure, the substrate analogue DHBT and solvent molecules were removed from the initial model. The rotation and the translation functions gave two clear single solutions, which corresponded to two molecules in the asymmetric unit.

These two molecules located in the asymmetric unit yielded a Matthews coefficient (V_M) of 2.41 Å^3/Da and a corresponding solvent content of 49.1%.[18] Both solutions were employed in the refinement procedure performed with CNS 1.1.[19]

From the total of independent reflections, 5% were used for calculating the R_{free} and thus monitor the progress of the refinement. After the first cycle of refinement, composed of a rigid-body and an energy minimization procedure, residues Gly61 to Ser74 for subunit A and residues Lys62 to Ile78 for subunit B of the HSV1-TK homodimer were reconstructed. Subsequently, several cycles (simulated annealing, energy minimization, and grouped temperature factor refinement) were performed and were interchanged with manual rebuilding sessions using the molecular graphics program O.[20]

Within the binding pocket of both subunits A and B of the HSV1-TK homodimer, a residual density was present in the ($F_{obs} - F_{calc}$) electron density map contoured at 2σ and was clearly identified as the substrate analogue N-Me DHBT. The sulfate ions were introduced also directly in the ATP-binding pocket. Water molecules were positioned progressively if they were observed in an environment susceptible to provide hydrogen bonds. In the final stages of the refinement, individual restrained *B*-factor refinement was performed.

Subsequently, the model of HSV1-TK complexed with the N-Me DHBT was used as a search probe to solve by molecular replacement with the program PHASER[17] the structure of HSV1-TK containing the fluorinated analogue N-Me FHBT. Iterative model refinement carried out with PHENIX[21] and manual building done with the program COOT[22] completed the structure of HSV1-TK:N-Me FHBT. Likewise, water molecules and sulfate ions were introduced at the end of the refinement procedure. A residual density

was present in the ($F_{obs} - F_{calc}$) electron density map contoured at 2.5σ and located in the active site of both subunits A and B. The LigandFit subroutine of PHENIX localized the N-Me FDHT derivative within this residual electron density map.[23,24] The eLBOW subroutine was used to generate the geometry restraint information of the N-Me FHBT derivative for performing the final refinement step with the introduced derivative.[25]

The stereochemical quality of the two final models was assessed with PROCHECK.[26] The coordinates and structure factors are deposited in the Protein Data Bank under the accession codes 3F0T and sf3f0t for HSV1-TK complexed with N-Me DHBT and under 3RDP and sf3rdp for HSV1-TK complexed with N-Me FHBT.

Figures 4–7 were produced with the program PyMOL (http://www.pymol.sourceforge.net; http://www.pymol.org).

RESULTS AND DISCUSSION

Docking Study Results

The choice of the docking program among the ones available (Autodock, Dock, GOLD, FlexX) was made based on a study of Kellenberger et al.[27] stating that both the capacity of reproducing the x-ray pose (accuracy) as well as the discrimination of known thymidine kinase inhibitors were best achieved with the docking program GOLD.

GOLD 2.2 (Genetic Optimisation for Ligand Docking) is especially suited for complexes displaying predominantly H-bonds.[28] Apart from visual inspection, the main parameter for estimating docking success is the fitness function, which has been optimized for the prediction of ligand binding poses rather than affinity. Docking studies were performed in order to investigate whether N-Me DHBT would, indeed, be a substrate for HSV1-TK. The docking model was tested by examining binding modes of thymidine, PCV, GCV, and DHBT. It was successfully validated since all binding modes corresponded to the binding modes seen in their respective crystal structures with HSV1-TK. Root mean square deviation (RMSD) values were always close to 1 Å.

The docking results predicted that N-Me DHBT would indeed be a HSV1-TK substrate since N-Me DHBT shows the same interactions known to thymidine and DHBT. Specifically, 3′-OH groups of the N-Me DHBT and N-Me FHBT point toward the catalytic center of the enzyme, formed by Glu83 and Arg163. Due to these interactions, it was predicted that N-Me DHBT and N-Me FHBT would undergo phosphorylation, since their hydroxyl functionalities mimic the 5′-hydroxyl group of thymidine as later confirmed by the x-ray structures reported here. The second OH group of N-Me DHBT (4′-OH) and the F atom of N-Me FHBT point towards the LID domain (residues

219–226) of HSV1-TK. Based on these results, both compounds fulfill the prerequisite for being HSV1-TK substrates.

Synthesis of N-Me DHBT

The synthesis of the key intermediate N-Me DHBT (Figure 2) was accomplished in analogy to published procedures with slight modifications in the work up.[29,30] The starting compound, 2,4-dihydroxy-5,6-dimethylpyrimidine (**1**), was converted to the corresponding chloride **2**, which was used without further purification. The treatment of **2** with sodium methanolate gave the dimethoxy compound **3** in 95% yield after purification by column chromatography. In parallel, 1,3-dibenzyloxy-2-propanol (**5**) was oxidized using Corey oxydation to yield ketone **6**. The product of the reaction between the lithiated compound **4** and ketone **6** was the C-6 substituted pyrimidine **7**. The removal of the tertiary hydroxyl group was accomplised using radical deoxygenation via oxalyl ester **8**. Introduction of the methyl group in the N-1 position of the pyrimidine ring was achieved by the reaction of **9** with methyl iodide. The cleavage of two benzyl protecting groups, followed by the removal of the methoxy group gave N-Me DHBT in 13% overall yield. The insertion of the methyl group on the N-1 compared to DHBT allows avoiding intramolecular cyclisation while performing fluorination on one of the OH groups for producing the ^{18}F labeled N-Me FHBT.

In Vitro Validation of N-Me DHBT as Substrate of HSV1-TK

In analogy to the previously published protocol,[6,9] we initially investigated whether N-Me DHBT would be phosphorylated by HSV1-TK. Prior to test the phosphorylation of N-Me DHBT, we always assessed HSV1-TK activity using thymidine and DHBT as positive controls. The formation of ADP and the monophosphorylated substrate, as well as the disappearance of the substrate over time, were clearly visible. The retention times of N-Me DHBT and ADP differed only by 0.2 minutes, making a clear distinction between the two components difficult. However, recording the UV spectra produced by the DAD (Diode Array Detector) allowed to detect the UV-maxima at 267 nm and 258 nm that corresponded to ADP and N-Me DHBT, respectively. The incubation of N-Me DHBT with HSV1-TK, also revealed the presence

TABLE 1 Enzyme kinetics data obtained by the spectrophotometric assay

Compound	N-Me DHBT	dT*	PCV*	DHBT*
K_m (μM)	10	0.2	1.5	35.3
k_{cat} (s^{-1})	0.036	0.35	0.05	0.035

*Data from the literature.[6,10]

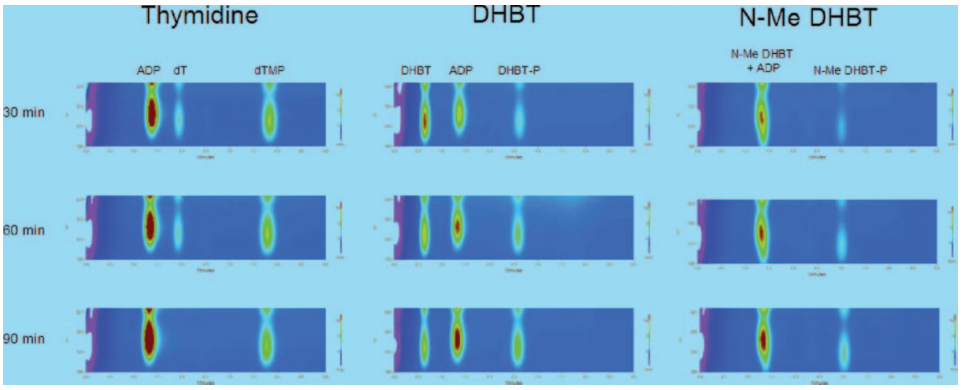

FIGURE 3 HPLC-based phosphorylation pattern assay. The formation of new peaks (ADP and monophosphorylated product) has been monitored by HPLC coupled to a diode array detector. To assess the functionality of the HSV1-TK enzyme, thymidine (dT) and DHBT were used as positive controls. These chromatograms clearly show the formation of ADP and the monophosphorylated products dTMP and DHBT-P, respectively. For N-Me DHBT, the formation of N-Me DHBT monophosphate (N-Me DHBT-P) is clearly visible, while the peaks of N-Me DHBT and ADP overlap. (Color figure available online.)

of a new peak at 7.05 minutes, which corresponded to the monophosphorylated N-Me DHBT (Figure 3). An increase over time of this newly formed peak provided another evidence that N-Me DHBT is indeed a substrate of HSV1-TK.

Determination of the Binding and Catalytic Constant of N-Me DHBT as Substrate of HSV1-TK

Quantative enzyme kinetics measurements to determine k_{cat} and K_m values were performed by a spectrophotometric assay using a previously published protocol.[9,10] The experiments, performed in triplicates, showed that N-Me DHBT was phosphorylated at a similar rate as FHBG ($K_m = 10 \pm 0.3\ \mu M$; $k_{cat} = 0.036 \pm 0.015\ sec^{-1}$) (see Table 1). Compared to DHBT ($K_m = 35.3 \pm 1.3\ \mu M$; $k_{cat} = 0.035 \pm 0.01\ sec^{-1}$), N-Me DHBT exhibits a rather similar K_m value, suggesting that the introduction of a methyl group at the N-1 position of the pyrimidine ring of DHBT has no dramatic influence on the binding affinity of N-Me DHBT.

Cell Proliferation Assay

Cell proliferation measurements were performed on B16F1 cells using the XTT proliferation assay protocol.[9] No inhibition of cell proliferation was observed for the HSV-1 TK transduced B16F1 cells (B16F1 HSV1-TK+) and B16F1 wildtype cells up to 500 μM. Cell proliferation was partially inhibited at 1 mM. The later concentration is significantly higher than the one where GCV shows high cytotoxicity.[9]

TABLE 2 Data collection and refinement statistics of the complexes HSV1-TK:N-Me DHBT and HSV1-TK:N-Me FHBT[a]

Data collection	HSV1-TK : N-Me DHBT	HSV1-TK : N-Me FHBT
Beamline	**SLS – X06SA**	**SLS – X06DA**
Resolution limits (Å)	31 – 2.0	35.3–2.8
No. of measured reflections	487690	60375
No. of unique reflections	48655	16788
Redundancy	10 (9.9)	3.6 (3.6)
Completeness (%)	100 (100)	91.3 (93)
$I/\sigma(I)$	17.6 (5.4)	5.9 (2.3)
R_{sym} (%)	11.1 (38.5)	18.6 (56.6)
Refinement and final model		
No. of reflections	48627	15969
No. of omitted reflections	2438	819
No. of proteins residues	630	634
No. of water molecules	303	81
No. of ions	6	3
No. of bound ligand	2	2
R (%)/R_{free} (%)	19.5/22.8	20/24.4
Mean on *B*-factors (Å^2)		
Protein/solvent	30.6/41	36.3/30
Compound	34	40.2
RMSD. from ideal geometry		
Bond length (Å)	0.006	0.002
Bond angles (°)	1.3	0.55

[a]Figures in parentheses correspond to the value for the highest shell of resolution (2.1–2.0 Å) for HSV1-TK:N-Me DHBT and (2.95–2.8 Å) for HSV1-TK:N-Me FHBT.

Overall Structure of HSV1-TK:N-Me DHBT

With the aim to improve the design of a PET-tracer harbouring better pharmacokinetics, the structure of HSV1-TK complexed with the substrate analogue N-Me DHBT was solved by molecular replacement at 2.0 Å resolution in order to gain insight into the binding mode of this new C-6-alkylated pyrimidine derivative within the nucleoside binding pocket. The structure of HSV1-TK:N-Me DHBT is a homodimer composed of the two subunits A and B. For several loops, due to their high mobility, the electron density map was discontinuous and, therefore, they could not be modeled. The final model of HSV1-TK:N-Me DHBT contains residues 45–147, 153–264, 280–373 in subunit A and residues 46–147, 153–220, 223–264, 274–374 in subunit B, where the missing residues 221 and 222 belong to the loop corresponding to the LID domain. In addition, the side chains of Met A130, Arg A293, Met B130, Met B179, Met B182, and Cys B362 were modeled with a double conformation. The relevant statistics of both data collection and model refinement are given in Table 2. The structure was refined to a R_{factor} of 19.5% and a R_{free} of 22.8%. The geometry analysis of the final model

revealed that most of the residues of the two subunits are located in the most favored regions of the Ramachandran plot, that is, 94.2% for the subunit A and 93% for the subunit B. Only one residue, Arg163, was found in the nonallowed region, although its main-chain geometry is in good agreement with the electron density map. This observation correlates with other HSV1-TK structures reported. The unfavorable geometry of Arg163 is due to its particular role: Arg163 participates in the phosphate transfer during the enzymatic reaction.

The overall α/β-fold of HSV1-TK:N-Me DHBT, which is composed of 12 α-helices and 7 β-sheets, is conserved compared to the previously solved HSV1-TK structures. The only noticeable difference appears in helix α1 at the residues Lys62-Ser74, following just the P-loop (residues Gly56–Gly61). Compared to most of the HSV1-TK structure that have been reported, either this helix α1 does not superimpose very well or is not fully constructed. For instance, the RMSD between the two subunits A and B of the HSV1-TK:N-Me DHBT is 0.96 Å.

Binding of the Substrate N-Me DHBT in the Nucleoside Binding Pocket

The position and orientation of the substrate N-Me DHBT in the thymidine binding pocket was clearly interpretable in the $(F_{obs} - F_{calc})$ electron density contoured at 2σ and both substrates for each subunit were introduced into the active site with no ambiguity.

The interactions of N-Me DHBT with the binding site are depicted in Figure 4. The structure reveals that the newly introduced N-methyl group

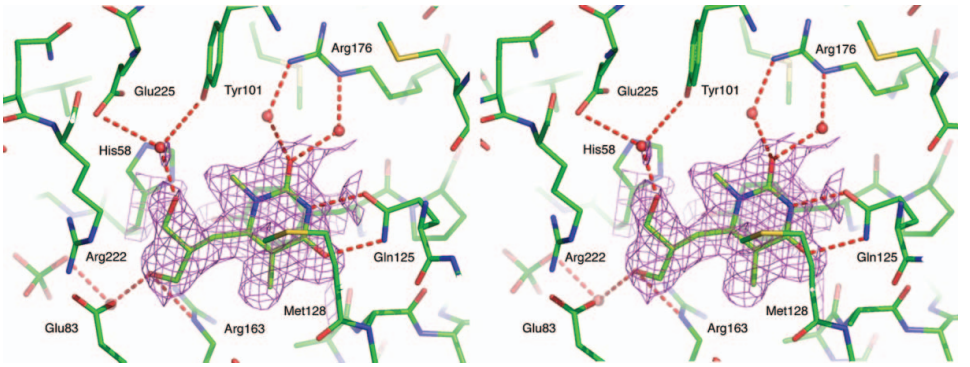

FIGURE 4 Stereo view of the interactions of N-Me DHBT with the active site of HSV1-TK. The $(3F_{obs} - 2F_{calc})$ electron density map at a resolution of 2.0 Å obtained at the end of the refinement is contoured at 1σ and colored in purple. The final HSV1-TK:N-Me DHBT model is superposed. The water molecules are depicted as red spheres and the hydrogen bonds are displayed as red dashed lines. The representation was done with the subunit A of the homodimer. (Color figure available online.)

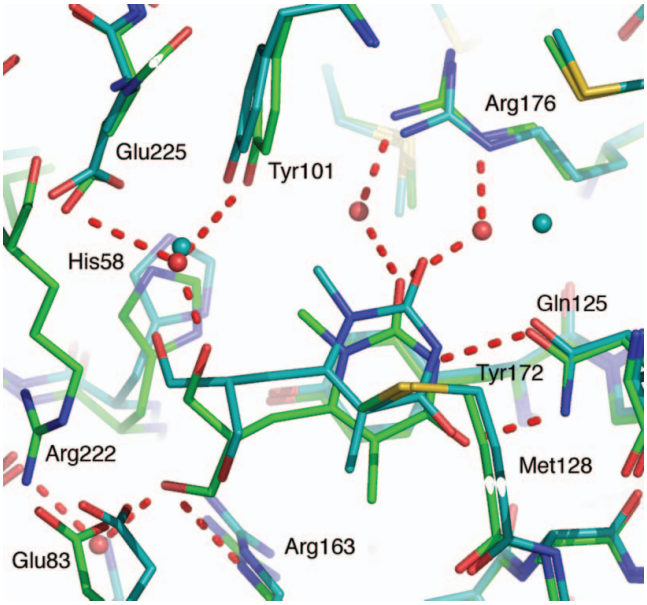

FIGURE 5 Superposition of the active sites of subunit A (colored in green) and subunit B (colored in red) of HSV1-TK:N-Me DHBT. The water molecules are displayed as blue spheres. The hydrogen bonds displayed as red dashed lines are shown for subunit A only. (Color figure available online.)

stabilizes the aliphatic moiety of the molecule due to its increased bulkiness. The interactions of the thymine moiety of N-Me DHBT with residues of the binding site are conserved (Figure 4).

First, the pyrimidine ring of the thymidine moiety is fixed between Met128 and Tyr172, forming a sandwich-like complex. The thymidine moiety is further held in place via a hydrogen bond network, which involves the carboxamide of Gln125, and the side chain of Arg176 and two water molecules.

The dihydroxy-isobutyl side chain of N-Me DHBT is maintained within the substrate active site by hydrogen bonds. The 3′-OH is connected via a hydrogen bond with the side chain of the catalytically important residue Arg163 (via the atom NE) and the sulfate ion via a water molecule. One new feature appears: A water molecule mediates interactions between the dihydroxy-isobutyl chain of N-Me DHBT (atom 4′-OH) and the side chains of residues Glu225 and Tyr101. Glu225 belongs to the LID domain, a lysine- and arginine-rich segment that is able to form a flap enclosing the active site.

As shown in Figure 5, this water molecule is also present in the subunit B connecting the 4′-OH of N-Me DHBT with the side chains of residues Glu225 and Tyr101 via hydrogen bonds. All the interactions between the N-Me DHBT substrate present in the active site of the subunit A are conserved in the subunit B of the homodimer. The two thymidine rings of the substrate

analogue are almost positioned at the same place. However, the dihydroxy-isobutyl side chain appears to be more flexible in the binding site of HSV1-TK.

Following the binding of N-Me DHBT to the active site, the LID domain (residues Lys219–Arg226) is in a closed conformation in both subunits. Nevertheless, in subunit B, the end of the loop (Gln221–Arg222) seems flexible and could not be modeled because the electron density map was not continuous.

Interestingly, in subunit A, residue Lys62 located by the helix α1 (Lys62–Ser74) is pointing outside of the ATP-binding pocket, whereas in subunit B, it is pointing in direction of the sulfate ion located in the ATP-binding pocket.

Differences in the Binding Mode Between HSV1-TK:N-Me DHBT and HSV1-TK:DHBT

The superposition between the active site of HSV1-TK:N-Me DHBT and HSV1-TK:DHBT (PDB entry code 1E2P) reveals that there are no relevant differences at the level of the backbone and of the side chains (Figure 6A). The only noticeable difference is located at the level of the helix α1 that does not superpose very well for each subunit. In this case also, residue Lys62 in subunit A of HSV1-TK:N-Me DHBT points out of the ATP-binding site whereas in subunit A of HSV1-TK:DHBT, it points towards the sulfate ion. Most of the interactions established in the active site by the substrate N-Me DHBT are conserved in the binding of DHBT. The thymidine ring is sandwiched between Met128 and Tyr172 and maintained in place by hydrogen bonds involving the side chains of Gln125 and Arg176. Likewise, the 3′-OH of the dihydroxy-isobutyl side chain of DHBT establishes hydrogen bonds with the side chain of Arg163 (via the atom NH2). However, there is no water molecule present between the 4′-OH of the dihydroxy-isobutyl side chain and the side chains of residues Glu225 and Tyr101 (Figure 6A). The dihydroxy-isobutyl side chain of DHBT appears to be also flexible.

Differences in the Binding Pattern Between HSV1-TK:N-Me DHBT and HSV1-TK:dT or HSV1-TK:dTMP:ADP

Figure 6B shows the differences in the binding pattern between HSV1-TK:N-Me DHBT and HSV1-TK:dTMP:ADP (PDB entry code 1VTK;[31] 2.75Å resolution). There are no relevant differences at the level of the backbone and the side chains of HSV1-TK:dTMP:ADP. The only difference is located at the level of the helices α1 that do not superpose well. The thymidine ring of dTMP is maintained in the nucleoside binding pocket by the same interactions that are established by the thymidine ring of N-Me DHBT. However, the dihydroxy-isobutyl side chains of N-Me DHBT and the side chain of dTMP do not occupy the same place. In the case of HSV1-TK:dTMP:ADP,

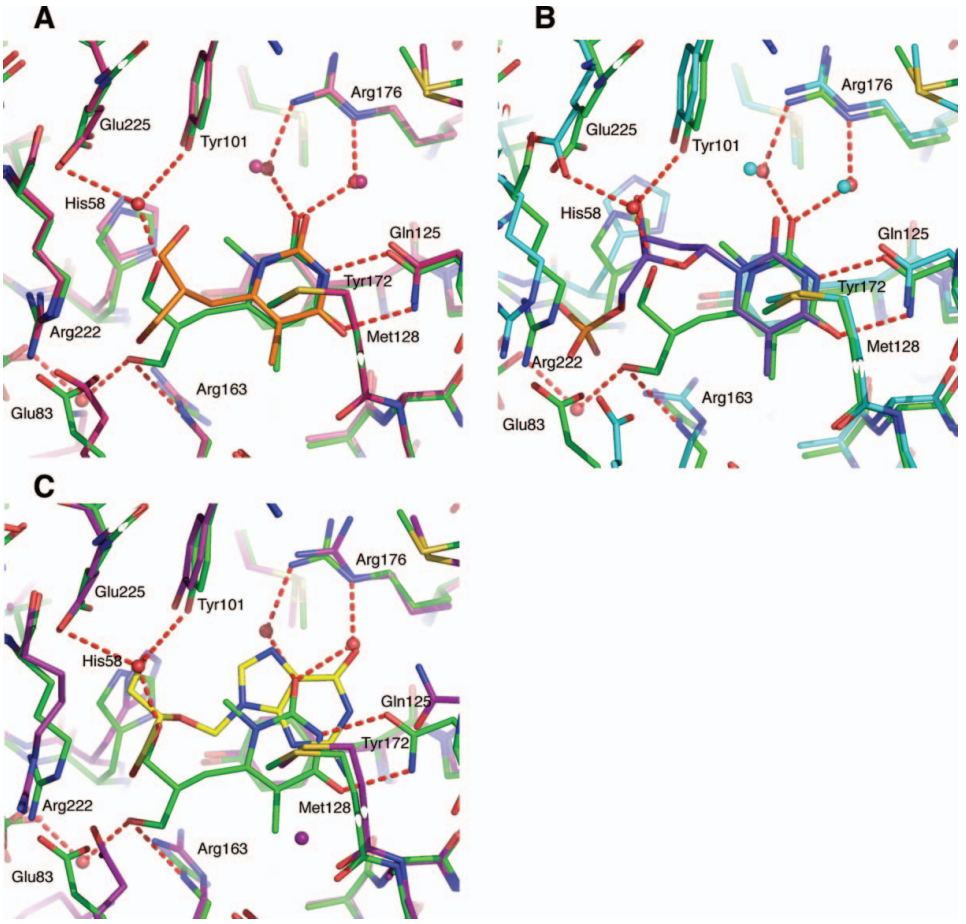

FIGURE 6 A) Superposition of the active sites of HSV1-TK:N-Me DHBT (colored in green) and HSV1-TK:DHBT (HSV1-TK is colored in dark pink and DHBT is colored in orange). B) Superposition of the active sites of HSV1-TK:N-Me DHBT (colored in green) and HSV1-TK:dTMP:ADP (HSV1-TK is colored in cyan and dTMP and ADP are dark blue). C) Superposition of the active sites of HSV1-TK:N-Me DHBT (colored in green) and HSV1-TK:ganciclovir (HSV1-TK is colored in purple and ganciclovir in yellow). The pictures are done with both subunits A of each homodimer. The hydrogen bonds, depicted as red dashed lines, are shown only for subunit A of HSV-1 TK complexed with N-Me DHBT. (Color figure available online.)

the 3′-OH of the ribose moiety of dTMP makes hydrogen bond interactions with the side chains of residues Glu225 and Tyr101. The position occupied by the 3′-OH of dTMP corresponds to the one occupied by the water molecule in the structure of HSV1-TK:N-Me DHBT, establishing hydrogen bonds between the 4′-OH atom and the residues Glu225 and Tyr101 (Figure 6B).

Differences in the Binding Mode Between HSV1-TK:N-Me DHBT and HSV1-TK in Complex with a Purine Substrate Analogue

Figure 6C depicts the differences in the binding pattern between HSV1-TK:N-Me DHBT and HSV1-TK:ganciclovir (PDB entry code 1KI2[32]).

The guanine moiety of ganciclovir and the thymidine moiety of N-Me DHBT occupy a different location with the nucleoside binding pocket of HSV1-TK. However, the binding mode observed for ganciclovir displays some similarities with the one of HSV1-TK:N-Me DHBT. The guanine moiety of ganciclovir is stacked between Met128 and Tyr172. The carboxamide of Gln125 forms hydrogen bonds with the atoms N1, N2 and O6 of the guanine moiety. The side chain of ganciclovir is hydrogen bonded to the side chains of Tyr101 and Glu225 via the 4′-OH atom. The position occupied by the 4′-OH atom of ganciclovir matches the one occupied by the water molecule in the structure of HSV1-TK:N-Me DHBT.

Binding of the Substrate N-Me FHBT in the Nucleoside Binding Pocket

The final model of HSV1-TK:N-Me FHBT solved at 2.8 Å resolution contains residues 46–264, 280–374 in subunit A and residues 46–264, 274–374 in subunit B. The relevant statistics of both data collection and model refinement are given in Table 2. The structure was refined to a R_{factor} of 20% and a R_{free} of 24.4%. The geometry analysis of the final model revealed that most of the residues of the two subunits are located in the most favored regions of the Ramachandran plot, 90.8% for the subunit A and 89.1% for the subunit B.

The N-Me FHBT derivative was clearly located in the thymidine binding pocket of the two subunits A and B of the HSV1-TK homodimer. The binding interactions of N-Me FHBT within the active site are depicted in Figure 7A. N-Me FHBT establishes mostly the same interactions as N-Me DHBT (Figure 7B). Likewise, the pyrimidine ring is inserted in a sandwich-like complex between Met128 and Tyr172. The thymidine moiety is kept in place by a hydrogen bond network, established with the side chains of Gln125 and of Arg176 and one water molecule. The acyclic side chain of N-Me FHBT is kept in the active site through hydrogen bonds: The 3′-OH atom is connected via hydrogen bonds with the side chain of the Arg163 (atom NE), the side chain of Glu83 (atom OE1) and a water molecule. The fluorine atom points in the direction of Glu225, Tyr101, and His58 and establishes no interactions. The interactions established by N-Me FHBT in the active site of the subunit A are also present in the subunit B of the homodimer. The additional water molecule found in the structure of HSV1-TK:N-Me DHBT is not present in the structure of HSV1-TK:N-Me FHBT. Upon the binding of N-Me FHBT

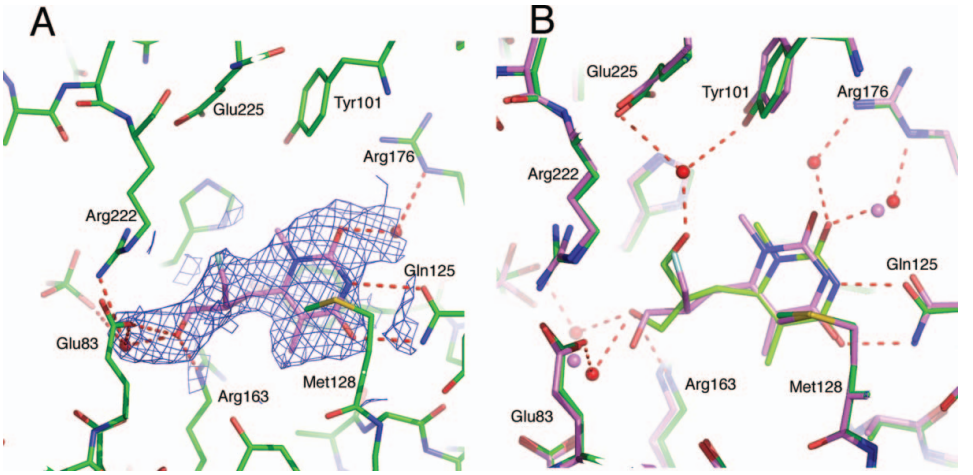

FIGURE 7 View of the binding interactions of N-Me FHBT within the active site of HSV1-TK. A) The $(2F_{obs} - F_{calc})$ electron density map at a resolution of 2.8 Å obtained at the end of the refinement is contoured at 1σ and colored in blue. The final HSV1-TK:N-Me FHBT model is superposed. N-Me FHBT is in sticks and colored in violet. The water molecules are depicted as red spheres and the hydrogen bonds are displayed as red dashed lines. The representation was done with the subunit A of the homodimer. B) Superposition of the active sites of HSV1-TK:N-Me DHBT (colored in green) and HSV1-TK:N-Me FHBT (colored in violet). Only the hydrogen bonds (red dashed lines) established by N-Me DHBT are displayed and the water molecules in the structure of HSV1-TK:N-Me DHBT are depicted as red spheres. The representation was done with the subunits A of the homodimer. (Color figure available online.)

to the active site, the LID domain (residues Lys219–Arg226) is in a closed conformation in both subunits.

The structure of HSV1-TK:N-Me FHBT revealed that the fluorine atom is not lost and that the internal cyclization of the acyclic side chain did not occur. It also confirmed that the fluorinated derivative N-Me FHBT is a putative substrate of HSV1-TK.

CONCLUSION

Molecular modeling was successfully employed to select a novel C-6 substituted pyrimidine derivative for the development as a PET ligand for gene expression monitoring. The introduction of a methyl group at the N-1 position of the pyrimidine ring did not have any dramatic effect on the binding properties of the methylated derivative. The novel lead compound, N-Me DHBT was shown to be a substrate for HSV1-TK besides being non-cytotoxic. The x-ray structure of HSV1-TK in complex with N-Me DHBT confirmed the molecular modeling prediction and gives new insights for the design and synthesis of further C-6 substituted pyrimidine derivative with improved pharmacokinetics. Likewise, the structure of HSV1-TK:N-Me FHBT confirmed that the fluorinated derivative is a possible substrate for HSV1-TK. While in vitro validation including cell uptake studies, as well as in vivo PET studies

are necessary to fully assess the biological properties of [^{18}F]N-Me FHBT for monitoring HSV1-TK expression in vivo, we expect that the radiosynthesis of [^{18}F]N-Me FHBT will be facilitated by the presence of the methyl group on N-1, preventing intramolecular cyclization observed with N-1-free C-6 pyrimidine derivatives such as DHBT and undesired side reactions.[6] According to the observation made for other C-6 pyrimidine derivatives,[6] the fluorinated derivative is expected to have similar biochemical properties as N-Me DHBT.

REFERENCES

1. Serganova, I.; Ponomarev, V.; Blasberg, R. Human reporter genes: potential use in clinical studies. *Nucl. Med. Biol.* **2007**, 34, 791–807.
2. Cai, H.; Yin, D.; Zhang, L.; Yang, X.; Xu, X.; Liu, W.; Zheng, X.; Zhang, H.; Wang, J.; Xu, Y.; Cheng, D.; Zheng, M.; Han, Y.; Wu, M.; Wang, Y. Preparation and biological evaluation of 2-amino-6-[18F]fluoro-9-(4-hydroxy-3-hydroxy-methylbutyl) purine (6-[18F]FPCV) as a novel PET probe for imaging HSV1-tk reporter gene expression. *Nucl. Med. Biol.* **2007**, 34, 717–725.
3. Tjuvajev, J. G.; Doubrovin, M.; Akhurst, T.; Cai, S.; Balatoni, J.; Alauddin, M. M.; Finn, R.; Bornmann, W.; Thaler, H.; Conti, P. S.; Blasberg, R. G. Comparison of radiolabeled nucleoside probes (FIAU, FHBG, and FHPG) for PET imaging of HSV1-tk gene expression. *J. Nucl. Med.* **2002**, 43, 1072–1083.
4. Iyer, M.; Barrio, J. R.; Namavari, M.; Bauer, E.; Satyamurthy, N.; Nguyen, K.; Toyokuni, T.; Phelps, M. E.; Herschman, H. R.; Gambhir, S. S. 8-[18F]Fluoropenciclovir: an improved reporter probe for imaging HSV1-tk reporter gene expression in vivo using PET. *J. Nucl. Med.* **2001**, 42, 96–105.
5. Johayem, A. *Development of novel nucleoside analogues for the PET imaging of herpes simplex virus type 1 thymidine kinase gene expression.* Ph. D. Thesis, Diss. ETH No.:15450, Eidgenössische Technische Hochschule Zürich, Switzerland, 2004.
6. Johayem, A.; Raic-Malic, S.; Lazzati, K.; Schubiger, P. A.; Scapozza, L.; Ametamey, S. M. Synthesis and characterization of a C6 nucleoside analogue for the in vivo imaging of the gene expression of herpes simplex virus type-1 thymidine kinase (HSV1 TK). *Chem Biodivers* **2006**, 3, 274–283.
7. Raic-Malic, S.; Johayem, A.; Ametamey, S. M.; Batinac, S.; De Clercq, E.; Folkers, G.; Scapozza, L. Synthesis, 18F-radiolabelling and biological evaluations of C-6 alkylated pyrimidine nucleoside analogues. *Nucleosides Nucleotides Nucleic Acids* **2004**, 23, 1707–1721.
8. Pilger, B. D.; Perozzo, R.; Alber, F.; Wurth, C.; Folkers, G.; Scapozza, L. Substrate diversity of herpes simplex virus thymidine kinase. Impact Of the kinematics of the enzyme. *J. Biol. Chem.* **1999**, 274, 31967–31973.
9. Schelling, P.; Claus, M. T.; Johner, R.; Marquez, V. E.; Schulz, G. E.; Scapozza, L. Biochemical and structural characterization of South methanocarba-thymidine that specifically inhibits growth of herpes simplex virus type 1 thymidine kinase transduced osteosarcoma cells. *J. Biol. Chem.* **2004**, 279, 32832–32838.
10. Schelling, P.; Folkers, G.; Scapozza, L. A spectrophotometric assay for quantitative determination of kcat of herpes simplex virus type 1 thymidine kinase substrates. *Anal. Biochem.* **2001**, 295, 82–87.
11. Jost, L. M.; Kirkwood, J. M.; Whiteside, T. L. Improved short- and long-term XTT-based colorimetric cellular cytotoxicity assay for melanoma and other tumor cells. *J. Immunol. Methods* **1992**, 147, 153–165.
12. Roehm, N. W.; Rodgers, G. H.; Hatfield, S. M.; Glasebrook, A. L. An improved colorimetric assay for cell proliferation and viability utilizing the tetrazolium salt XTT. *J. Immunol. Methods* **1991**, 142, 257–265.
13. Fetzer, J.; Michael, M.; Bohner, T.; Hofbauer, R.; Folkers, G. A fast method for obtaining highly pure recombinant herpes simplex virus type 1 thymidine kinase. *Protein Expr. Purif.* **1994**, 5, 432–441.
14. Vogt, J.; Perozzo, R.; Pautsch, A.; Prota, A.; Schelling, P.; Pilger, B.; Folkers, G.; Scapozza, L.; Schulz, G. E. Nucleoside binding site of herpes simplex type 1 thymidine kinase analyzed by x-ray crystallography. *Proteins* **2000**, 41, 545–553.

15. Leslie, A. G. The integration of macromolecular diffraction data. *Acta Crystallogr. D Biol. Crystallogr.* **2006**, 62, 48–57.
16. Evans, P. Scaling and assessment of data quality. *Acta. Crystallogr. D Biol. Crystallogr.* **2006**, 62, 72–82.
17. McCoy, A. J.; Grosse-Kunstleve, R. W.; Storoni, L. C.; Read, R. J. Likelihood-enhanced fast translation functions. *Acta. Crystallogr. D Biol. Crystallogr.* **2005**, 61, 458–464.
18. Matthews, B. W. Solvent content of protein crystals. *J. Mol. Biol.* **1968**, 33, 491–497.
19. Brunger, A. T.; Adams, P. D.; Clore, G. M.; DeLano, W. L.; Gros, P.; Grosse-Kunstleve, R. W.; Jiang, J. S.; Kuszewski, J.; Nilges, M.; Pannu, N. S.; Read, R. J.; Rice, L. M.; Simonson, T.; Warren, G. L. Crystallography & NMR system: A new software suite for macromolecular structure determination. *Acta Crystallogr. D Biol. Crystallogr.* **1998**, 54, 905;921.
20. Jones, T. A.; Zou, J. Y.; Cowan, S. W.; Kjeldgaard, M. Improved methods for building protein models in electron density maps and the location of errors in these models. *Acta Crystallogr. A.* **1991**, 47, 110–119.
21. Adams, P. D.; Grosse-Kunstleve, R. W.; Hung, L. W.; Ioerger, T. R.; McCoy, A. J.; Moriarty, N. W.; Read, R. J.; Sacchettini, J. C.; Sauter, N. K.; Terwilliger, T. C. PHENIX: building new software for automated crystallographic structure determination. *Acta Crystallogr. D Biol. Crystallogr.* **2002**, 58, 1948–1954.
22. Emsley, P.; Cowtan, K. Coot: model-building tools for molecular graphics. *Acta Crystallogr. D Biol. Crystallogr.* **2004**, 60, 2126–2132.
23. Terwilliger, T. C.; Adams, P. D.; Moriarty, N. W.; Cohn, J. D. Ligand identification using electron-density map correlations. *Acta Crystallogr. D Biol. Crystallogr.* **2007**, 63, 101–107.
24. Terwilliger, T. C.; Klei, H.; Adams, P. D.; Moriarty, N. W.; Cohn, J. D. Automated ligand fitting by core-fragment fitting and extension into density. *Acta Crystallogr. D Biol. Crystallogr.* **2006**, 62, 915–922.
25. Moriarty, N. W.; Grosse-Kunstleve, R. W.; Adams, P. D. electronic Ligand Builder and Optimization Workbench (eLBOW): a tool for ligand coordinate and restraint generation. *Acta Crystallogr. D Biol. Crystallogr.* **2009**, 65, 1074–1080.
26. Laskowski, R. A.; Moss, D. S.; Thornton, J. M. Main-chain bond lengths and bond angles in protein structures. *J. Mol. Biol.* **1993**, 231, 1049–1067.
27. Kellenberger, E.; Rodrigo, J.; Muller, P.; Rognan, D. Comparative evaluation of eight docking tools for docking and virtual screening accuracy. *Proteins* **2004**, 57, 225–242.
28. Jones, G.; Willett, P.; Glen, R. C.; Leach, A. R.; Taylor, R. Development and validation of a genetic algorithm for flexible docking. *J. Mol. Biol.* **1997**, 267, 727–748.
29. Hsu, L.-Y.; Wise, D. S.; Kucera, L. S.; Drach, J. C.; Townsend, L. B. Synthesis of Anti-Restricted pyrimidine acyclic Nucleosides. *J. Org. Chem.* **1992**, 57, 3354–3358.
30. Hsu, L.-Y.; Wise, D. S.; Shannon, W. M.; Drach, J. C.; Townsend, L. B. Synthesis of C-6 pyrimidine acyclic nucleoside analogs as potential antiviral agents. *Nucleosides Nucleotides* **1994**, 13, 563–584.
31. Wild, K.; Bohner, T.; Folkers, G.; Schulz, G. E. The structures of thymidine kinase from herpes simplex virus type 1 in complex with substrates and a substrate analogue. *Protein Sci.* **1997**, 6, 2097–2106.
32. Champness, J. N.; Bennett, M. S.; Wien, F.; Visse, R.; Summers, W. C.; Herdewijn, P.; de Clerq, E.; Ostrowski, T.; Jarvest, R. L.; Sanderson, M. R. Exploring the active site of herpes simplex virus type-1 thymidine kinase by x-ray crystallography of complexes with aciclovir and other ligands. *Proteins* **1998**, 32, 350–361.